Mathematical Investigation and CFD Simulation of Monolith Reactors: Catalytic Combustion of Methane

Maryam Ghadrdan[*,1], Hamid Mehdizadeh[2]
[1]Department of Chemical Engineering, Norwegian University of Science and Technology (NTNU), N-7491 Trondheim, Norway
[21]Department of Chemical Engineering, Tarbiat Modares University, Tehran, Iran, P.O.Box: 14115-111
*Corresponding author: ghadrdan@chemeng.ntnu.no

Abstract: The goal of this work is to develop a two-phase (gas & solid) transient catalytic combustor model using a simplified flow field inside a single channel to test the advantages of COMSOL Multiphysics software. The flow field model includes axial convective transport with transverse energy and mass exchange via heat and mass transfer correlations. The solid is a thermally thin shell along which finite-rate heat conduction occurs in the axial direction. It is also shown that the Nusselt number does not correlate with Graetz number but rather depends on the such variables as gas velocity, inlet temperature and reactant concentration.

Keywords: Monolith reactor, Catalytic combustion, Methane.

1. Introduction

The interest in production of hydrogen from hydrocarbons has grown significantly recently. In order to achieve high surface to volume ratio with reasonable pressure drop, a usual reactor configuration are the monoliths (1). A number of studies have focused on the use of monolith reactors for catalytic combustion reactions using various numerical techniques (2-5). Finite element methods offer significant advantages over other methods, most notably in the ease with which flux boundary conditions may be implemented and the easy use of unstructured gridding methods (6) which is needed because of strong temperature and concentration gradients.

Models of catalytic monoliths often use a single channel to characterize the behavior of the entire monolith since every channel within a monolith structure should behave alike. There are, of course, exceptions. Researchers have explored heat loss effects near the periphery (7, 8) and non-uniform feed effects (9). In general, however, it is simpler and very reasonable to study monolith behavior using a single channel model.

The objective of this paper is to develop a finite element model for the simulation of a single channel of a catalytic monolith reactor using COMSOL Multiphysics software. Catalytic combustion of methane was selected as the model reaction. Here, some of the advantages of using COMSOL for CFD calculations are listed (10):

- It has an integrated modeling environment.
- It takes a semi-analytic approach: You specify equations, COMSOL symbolically assembles FEM matrices and organizes the bookkeeping.
- COMSOL is built on top of MATLAB, so user defined programming for the modeling, organizing the computation, or the post-processing has full functionality.
- It provides pre-built templates as Application Modes
- It provides multi-physics modeling linking well known “application modes” transparently.
- COMSOL innovated extended multi-physics-coupling between logically distinct domains and models that permits simultaneous solution.

2. Model

A circular monolith channel is considered in this paper, as shown in Figure 1. The three dimensional model is computation-ally prohibitive. The geometry of the model is an axisymmetric two dimensional geometry. The foam metal layer contains catalytically active element(s) can enhance the mass transfer both for the external mass transfer and the diffusion within layer.

The interaction between porous layer and the fluid is modeled by Brinkman formulation. The simulation parameters are derived from literature (11, 12) and are shown in tables 1-3. The Navier-Stokes equations are used to describe the flow regime in the bulk phase.

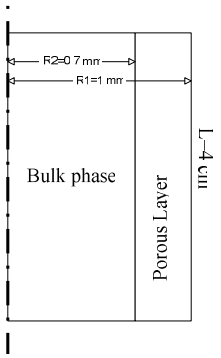

Figure 1. Schematic of the model

$$\frac{\partial \rho u}{\partial z} + \frac{1}{r}\frac{\partial (\rho v)}{\partial r} = 0 \quad (1$$

$$\rho u\frac{\partial u}{\partial z} + \rho v\frac{\partial (u)}{\partial r} = -\frac{\partial p}{\partial z} + \frac{\partial}{\partial z}\left[2\mu\frac{\partial u}{\partial z} - \frac{2}{3}\mu\nabla.V\right] + \frac{1}{r}\frac{\partial}{\partial r}\left[\mu r\left(\frac{\partial v}{\partial z} + \frac{\partial u}{\partial r}\right)\right] \quad (2$$

$$\rho u\frac{\partial v}{\partial z} + \rho v\frac{\partial (v)}{\partial r} = -\frac{\partial p}{\partial z} + \frac{\partial}{\partial z}\left[\mu\left(\frac{\partial v}{\partial z} + \frac{\partial u}{\partial r}\right)\right] + \frac{\partial}{\partial z}\left[2\mu\frac{\partial v}{\partial r} - \frac{2}{3}\mu\nabla.V\right] + \frac{2\mu}{r}\frac{\partial}{\partial r}\left[\frac{\partial v}{\partial z} - \frac{v}{r}\right] \quad (3$$

$$\rho u\frac{\partial Y_k}{\partial z} + \rho v\frac{\partial Y_k}{\partial r} = \left(\frac{\partial J_{k,z}}{\partial z} + \frac{1}{r}\frac{\partial (rJ_{k,z})}{\partial r}\right) + \dot{\omega}_k W_k \quad (4$$

$$(k = 1, ..., K_g)$$

$$\rho c_p\left(u\frac{\partial T}{\partial z} + v\frac{\partial T}{\partial r}\right) = \left(u\frac{\partial p}{\partial z} + v\frac{\partial p}{\partial r}\right) + \frac{\partial}{\partial z}\left(\lambda\frac{\partial T}{\partial z}\right) + \frac{\partial}{\partial r}\left(r\lambda\frac{\partial T}{\partial r}\right) - \sum_{k=1}^{K} c_{pk}\left(J_{kz}\frac{\partial T}{\partial z} + J_{kr}\frac{\partial T}{\partial r}\right) - \sum_{k=1}^{K} h_k\dot{\omega}_k W_k \quad (5$$

The boundary conditions presented in the figure above, are the following:

1) At the inlet of the channel:

$$T.n = T_0 \quad (6$$

$$c_A.n = c_{A0} \quad (7$$

$$v.n = v_0 \quad (8$$

2) At the axisymmetric line of the channel: Axial symmetry for all parameters

3) At the outlet of the channel: Convective flux is assumed

4) At the wall
No slip condition is assumed

Table 1. Simulation parameters for the bulk phase

Conditions	Bulk Phase
Reaction rate	$3\times10^{8} e^{\left(\frac{-90000}{RT}\right)} C_A$
Diffusivity	$D_1 = 9.99\times10^{-5}\times(T^{1.75}/P)$
Thermal conductivity	$k = 1.679\times10^{-2} + 5.073\times10^{-5}T$
Viscosity	$7.701\times10^{-6} + 4.166\times10^{-8}T$ $-7.531\times10^{-12}T^2$

Table 2. Simulation parameters for the porous layer

Conditions	Porous layer
Reaction rate	0
Diffusivity	$D_1\times(\varepsilon/\tau)$
Thermal conductivity	$\frac{k_2}{k_1} = \left(\frac{k_s}{k_1}\right)^{0.28-0.757\log\varepsilon-0.057\log(k_s/k_1)}$
Viscosity	$7.701\times10^{-6} + 4.166\times10^{-8}T$ $-7.531\times10^{-12}T^2$

In a catalytic combustor, combustion reactions may occur

1. in/on a catalyst layer, and
2. in the gas phase, if conditions are suitable to initiate and sustain homogeneous reactions.

It is important to recognize that both of these can occur simultaneously and that the reaction mechanisms are different although interactions may exist between the two.

The homogeneous gas phase combustion reaction are represented in simplified form as

$$CH_4 + 2O_2 \rightarrow CO_2 + 2H_2O \quad (9$$

$$\Delta H_{reac} = 802368 + 0.0133T^2 - 14.625T \quad (10$$

It is a gross simplification of the reaction scheme that may be taking place, e.g. in (13) there are a total of 149 reactions listed.

Table 3. Simulation conditions

Geometrical Conditions	
Channel length (m)	0.04
Porous layer thickness (mm)	1.0
Catalyst support materials	
Tortuosity, τ	4
Porosity, ε	0.4
Permeability, K m^2	1×10^{-8}
Thermal conductivity, k_s W/mK	25
Heat capacity, C_{ps} $J/kg.K$	900
Density, ρ_s kg/m^3	7870

3. Results and Discussions

Figures 2-4 show the typical concentration, temperature and velocity profiles in the axial direction of a single monolith reactor.

As the fuel (CH_4) and air flow down the channel, the reactants, CH_4 and O_2 are transported to the catalyst surface where they diffuse into the porous structure and react on catalytically active sites. The products from the reaction then diffuse through the porous structure and back into the gas phase as it continues to flow down the channel.

As the combustion reaction proceeds in the catalyst layer, energy is released and this is accompanied by a rise in temperature. As the temperature of the catalyst layer is higher than that of the bulk gas, energy is transferred by convection and the temperature of the gas increases in the axial direction. Energy exchange also occurs in the walls of the structure in the axial direction by conduction, and between the walls by radiation. The role that the catalyst is playing may be enhancing or inhibiting gas phase reactions.

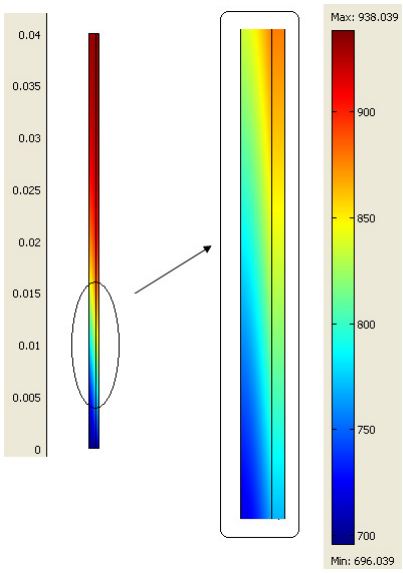

Figure 2. Temperature profile along the channel

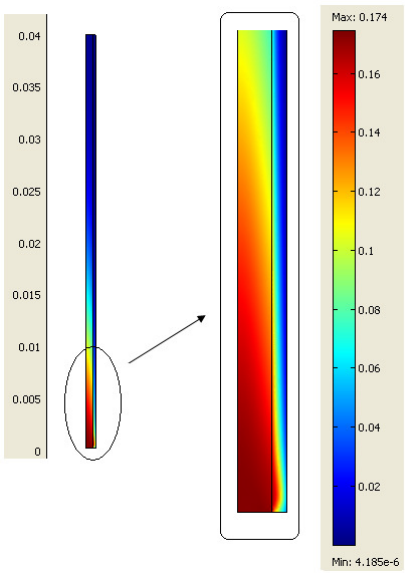

Figure 3. Concentration profile along the channel

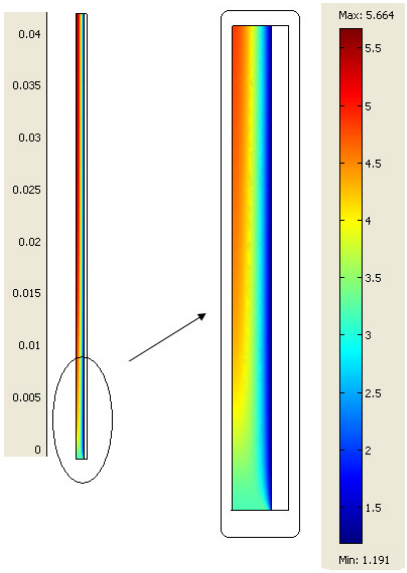

Figure 4. Velocity profile in the bulk phase

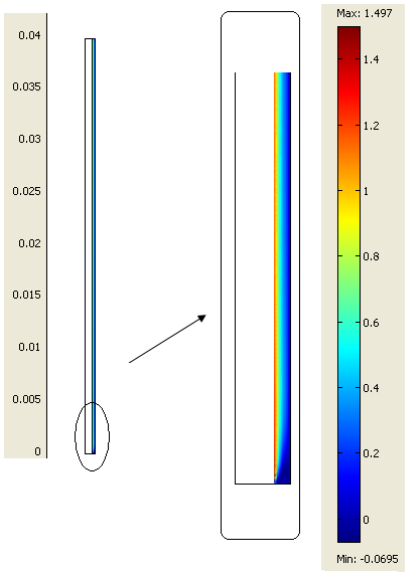

Figure 5. Velocity profile in the porous layer

A summary of simulations for different conditions is presented in table 4. It is obvious that there should be a logical set of input parameters to avoid hot spots in the reactor wall. However, the input data affect the conversion; especially in the case the longitude of the channel is not high enough.

Table 4. Summary of conditions in the simulations

Case	C_0 (mol/lit)	T_{in} (K)	V_{in} (m/s)	T_{out} (K)	Nu
1	0.001	700	1	725.1	4.21
2	0.01	700	1	932.1	3.87
3	0.001	800	1	810.6	4.13
4	0.01	800	1	990.2	3.69
5	0.001	700	3	720.5	4.24
6	0.01	700	3	846.5	4.47
7	0.001	800	3	827.3	4.12
8	0.01	800	3	899.2	4.35

The Nusselt number definition is as below:

$$Nu = \frac{Convective\ heat\ transfer}{Conductive\ heat\ transfer} \quad (11$$

This number is calculated by sketching the convective and conductive heat fluxes in the post-processing modes of COMSOL software. The Nusselt values in table 4 affirm the new claims that neither of the boundary conditions of constant wall temperature and constant wall flux represents the actual boundary condition.

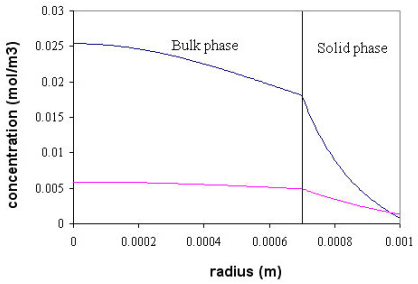

Figure 6. Concentration profile for cases 1 (up) and 2 (down)

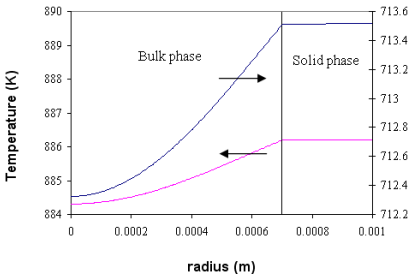

Figure 7. Temperature profile for cases 1 (up) and 4 (down)

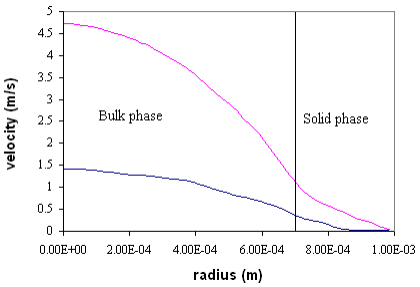

Figure 8. Velocity profile for cases 1 (up) and 4 (down)

Figures 6-8 show the temperature, velocity and concentration profiles at the axial location of 0.01 m for the initial values shown in table 4. Each profile is sketched for two different input parameters. The break point which is delineated by a vertical line is the intersection of the bulk and catalyst phases. A retarded viscous flow exists in the catalytic layer.

4. Conclusions

The results obtained from the 2-dimensional simulator for catalytic combustion of methane in a monolithic reactor are shown for different input parameters in the paper. They are theoretically acceptable. The effect of different input parameters on the Nusselt number is also investigated. It is shown that it can not be calculated by the common boundary conditions of constant wall temperature or constant wall flux.

5. References

1. Geus, J. W., and Giezen, J. C. V., Monoliths in catalytic oxidation, Catalysis Today, 47, 169 (1999).
2. P. Canu, and Vecchi, S., CFD Simulation of Reactive Flows: Catalytic Combustion in a Monolith, AIChE Journal, 48 (2002).
3. Quanli Zhu, Xutao Zhao, and Deng, Y., Advances in the Partial Oxidation of Methane to Synthesis Gas, Journal of Natural Gas Chemistry 13, 191 (2004).
4. Groppi, G., Belloli, A., Tronconi, E., and Forzatti, P., A comparison of lumped and distributed models of monolith catalytic combustors, Chemical Engineering Science, 50, 2705 (1995).
5. Hui Liu, Jundong Zhao, Chengyue Li, and Ji, S., Conceptual design and CFD simulation of a novel metal-based monolith reactor with enhanced mass transfer, Catalysis Today 105, 401 (2005).
6. Krummenacher, J. J., West, K. N., and Schmidt, L. D., Catalytic partial oxidation of higher hydrocarbons at millisecond contact times: decane, hexadecane, and diesel fuel, Journal of Catalysis, 215, 332 (2003).
7. Ablow, C. M., and Wise, H., Theoretical-Analysis of Catalytic Combustion in a Monolith Reactor, Combustion Science and Technology, 21, 35 (1979).
8. Schwiedernoch, R., Tischer, S., Correa, C., and Deutschmann, O., Experimental and Numerical Study on the Transient Behavior of Partial Oxidation of Methane in a Catalytic Monolith, Chemical Engineering Science, 58, 633 (2003).
9. Zygourakis, K., Transient Operation of Monolith Catalytic-Converters - a Two-Dimensional Reactor Model and the Effects of Radially Nonuniform Flow Distributions, Chemical Engineering Science, 44, 2075 (1989).
10. Guran, A., M. Cloud, and Zimmerman, W. B., Process Modelling and Simulation with Finite Element Methods, World Scientific Publishing Co. (2004).
11. R.E. Hayes, and Kolaczkowski, S. T., A study of Nusselt and Sherwood numbers in a monolith reactor, Catalysis Today, 47, 295 (1999).
12. Kaviany, M., Principles of Heat Transfer in Porous Media (Probability and Its Applications) Springer-Verlag, Berlin (1995).
13. M. Frenklach, H. Wang, and M.J. Rabinowitz, Optimization and Analysis of Large Chemical Kinetic Mechanisms Using the Solution Mapping Method-Combustion of Methane, *Prog. Energy Combust. Sci., 18*, 47 (1992).